A NOVEL CYLINDRICAL CAPACITIVE SENSOR (CCS) FOR BOTH RADIAL AND AXIAL MOTION MEASUREMENT

Hyeong-Joon Ahn, Il-Hae Kim, Dong-Chul Han
Seoul National University, AMED Laboratory
Department of Mechanical and Aerospace Engineering, Seoul, 151-744 ,Korea
ahj@amed.snu.ac.kr

ABSTRACT

This paper proposes a novel cylindrical capacitive sensor (CCS) for both radial and axial motion measurement. The proposed CCS has almost the same geometric configuration as the conventional CCS and the unused axial area of the CCS is utilized to measure the axial motion of a rotor, which can reduce complexity of the hardware configuration and offer more degree of freedom in design. First, a theoretical model of the proposed CCS considering the nonlinear characteristic of the CCS is derived. Based on the derived theoretical model, a simple compensation method to decouple the radial and axial motion measurements is proposed. In addition, error analysis is performed and a design rule is proposed to guarantee the same accuracy in measuring both radial and axial motion. Finally, a test rig and electronics for the proposed CCS are built and the performances of the proposed CCS is verified experimentally.

INTRODUCTION

A fully levitated five-axis AMB system usually needs independent four radial and one axial sensors. Hence, enough axial space for the radial and axial sensors is needed, which lower natural frequency of the AMB rotor. Therefore, a conical sensor can be used to reduce system complexity and improve the system dynamic characteristics. However, the conical sensor may cause a coupling problem in measuring the radial and thrust motion, and it is not easy to install and calibrate the conical sensor due to its geometry.

The probe-type displacement sensors most widely used are very sensitive to the surface quality of a rotor. They require additional algorithms to detect and compensate for the unnecessary signal induced by geometric errors. As an alternative to probe-type sensors, cylindrical capacitive sensor (CCS) was developed and applied to several applications since the CCS has low sensitivity to geometric errors and high resolution with large sensing area. It was verified that the CCS has much better performance in rejecting the geometric errors of a rotor than probe-type sensors [1] and can minimize the effects of geometric errors by changing the sensor angular size [2].

This paper proposes a novel CCS for both radial and axial motion measurement, which afford more compact design and system complexity reduction. A theoretical model of the new CCS considering the nonlinear characteristic of the CCS is derived and several analyses are performed. Based on the derived theoretical model, a simple compensation method to decouple the radial and axial motion measurements is proposed. In addition, error analysis of the proposed CCS is performed and a design rule is developed to guarantee the same accuracy in both radial and axial motion measurements. Finally, a test rig and electronics for the proposed CCS are built and the performances of the proposed CCS is verified experimentally. The proposed CCS can reduce complexity of the hardware configuration and offer more degree of freedom in system design.

CCS

Capacitive sensors are widely used in short-range ultra-precision and control applications because they have higher resolution than other type of sensors. The existing 4-segment CCS maximizes its sensing area to achieve as high resolution as possible, as shown in Fig. 1 (a). The rotor displacements can be approximated with Eq. (1) using the capacitances of four sensing electrodes (C_1, C_2, C_3, C_4).

$$X_{CCS4} = gain(C_1 + C_4 - C_2 + C_3),$$
$$Y_{CCS4} = gain(C_1 + C_2 - C_3 - C_4) \quad (1)$$

Although the 4-segment CCS has a high resolution, it is sensitive to odd harmonic errors, especially the 3rd harmonic component in geometric errors of a rotor. To overcome this shortcoming of the 4-segment CCS, Jeon et al. [2] proposed a new

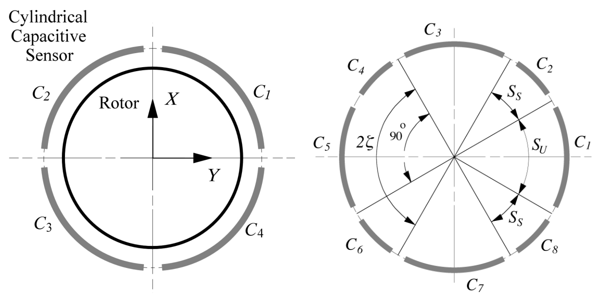

(a) 4-segment CCS (b) 8-segment CCS

Figure 1: The CCSs

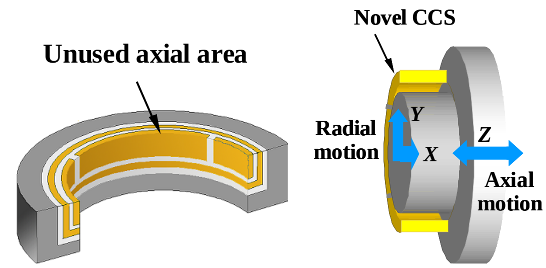

(a) Cross-section of a CCS (b) the propose CCS

Figure 2: Idea of the proposed CCS

configuration of CCS, that is, the 8-segment CCS, which consists of four shared and four unshared sensor segments, as shown in Fig. 1 (b). Total angular size 2ζ of a sensor unit is the sum of two shared and one unshared sensor segments.

$$2\zeta = 2S_S + S_U \tag{2}$$

Here S_S and S_U are the angular sizes of the shared and unshared segments, respectively.

The measured rotor displacements can be approximated by Eq. (3).

$$X_{CCS8} = gain(C_8 + C_1 + C_2 - C_4 - C_5 - C_6),$$
$$Y_{CCS8} = gain(C_2 + C_3 + C_4 - C_6 - C_7 - C_8) \tag{3}$$

The 8-segment CCS can possess an arbitrary angular size of the sensor unit through adjusting the angular sizes of the sensor segments and a proper angular size of a sensor unit can minimize the effects of geometric errors.

A NOVEL CCS FOR BOTH RADIAL AND AXIAL MOTION MEASUREMENT

Figure 2 (a) shows the cross-section of a CCS and there is unused axial area of the CCS. The idea of the novel CCS is that the axial area of the CCS can be used to measure axial motion as shown in Fig. 2 (b). If this idea is successfully implemented, more compact design and system complexity reduction can be achieved through removing axial sensor.

In case of the proposed CCS, capacitance of each electrode can be divided into two terms: axial and radial capacitances such as Eq. (4). Radial displacements can be approximated using the same equations as Eqs. (1) and (3) since the capacitances of the axial sensing area C_{ia} are removed due to differential configuration of the CCS.

$$C_i = C_{ir} + C_{ia} \tag{4}$$

Here, C_{ia} is capacitance of the axial area and C_{ir} is capacitance of the radial area.

If the radial thickness of the sensing electrode is t and the axial gap is δ_a, the sum of the capacitance of axial area can be expressed by

$$\sum_i C_{ia} = \varepsilon \frac{2\pi(b + t/2)t}{\delta_a} \tag{5}$$

Therefore, the axial motion may be expressed by the sum of all capacities like 6), if the sum of capacitance of radial area C_{ir} would be constant. However, as the rotor goes far from the center of the CCS, the sum of capacitances of the radial area (total capacitance) varies significantly according to the radial position of the rotor. It is necessary to investigate the radial position dependency of the total capacitance.

$$1/Z = \sum_i C_i - C_{offset} \tag{6}$$

Here, C_{offset} is the capacity due to raidal and stray capacitances.

The small capacitance of radial area of the CCS can be approximated as [1]

$$\Delta C \simeq \frac{\varepsilon b w}{\delta - \alpha\cos(\theta - \beta)} \Delta\theta \tag{7}$$

Here, b is sensor radius, w is sensor axial width, δ is radial gap between the sensor and the rotor, α is the eccentricity of rotor and β is the phase angle of the rotor eccentricity.

Nonlinear dependency of the sum of all capacities on the radial position of the rotor can be calculated through integrating (7) from 0 to 2π using integral table [3].

$$C_{0\ldots 2\pi} = \int_0^{2\pi} \Delta C = \frac{2\pi\varepsilon bw}{\delta} \frac{1}{\sqrt{1-(\frac{\alpha}{\delta})^2}} \quad (8)$$

As the rotor goes close to the CCS, the nonlinear characteristic becomes severe. In case of AMB, clearance of a back-up bearing is assumed as 75% of the nominal clearance and the total capacitance varies over 150%. Therefore, we cannot use the sum of capacitances directly to represent the axial motion.

To overcome the coupling between radial and axial measurements of the CCS, a simple compensation method using the measured X and Y displacements of the CCS will be presented later. Therefore, it is necessary to analyze the nonlinear characteristic of radial motion measurement of the CCS.

Nonlinear analysis of the CCS

Measured displacement in X direction using a CCS of angular size 2 ξ can be expressed as

$$X_{CCS} = \int_{-\xi}^{\xi} \Delta C - \int_{\pi-\xi}^{\pi+\xi} \Delta C \quad (9)$$

The small capacitance (7) can be expressed using power series by

$$\Delta C \simeq \frac{\varepsilon bw}{\delta} \sum_{n=0}^{\infty} \Big(\frac{\alpha}{\delta}\cos(\theta-\beta)\Big)^n \Delta\theta \quad (10)$$

Substituting Eq. (10) into Eq. (9) and simplifying, the solution exist only if n = even.

$$X_{CCS} = \frac{2\varepsilon bw}{\delta} \int_{-\xi}^{\xi} \sum_{l=0}^{\infty} \Big(\frac{\alpha}{\delta}\Big)^{2l+1} \cos^{2l+1}(\theta-\beta)\Delta\theta \quad (11)$$

Using following trigonal formula Eq. (12) and simplifying the equations, the resulting measured displacement of the rotor can be expressed as Eq. (13).

$$\cos^{2l+1}\vartheta = \frac{1}{4^l}\sum_{k=0}^{l} \binom{2l+1}{k} \cos{(2l+1-2k)\vartheta} \quad (12)$$

$$X_{CCS} = 8\frac{\varepsilon bw}{\delta} \sum_{l=0}^{\infty} \Big(\frac{\alpha}{2\delta}\Big)^{2l+1} \sum_{k=0}^{l} \binom{2l+1}{k} \frac{\sin{(2l+1-2k)\xi}}{2l+1-2k} \cos{(2l+1-2k)\beta} \quad (13)$$

The biggest nonlinear harmonic error is the third harmonics. However, if ξ is 60^o, the third harmonic phase error is removed, which means that the 8-segment CCS has minimal harmonic errors. In addition, the nonlinear gain of the radial motion measurement of the CCS can be evaluated through summing the first harmonic terms.

$$X_{CCS}^1 = 8\frac{\varepsilon bw}{\delta} \sum_{l=0}^{\infty} \Big(\frac{\alpha}{2\delta}\Big)^{2l+1} \binom{2l+1}{l} \sin\xi\cos\beta \quad (14)$$

Equation (14) can be simplified using a power series (15) and the resulting nonlinearity of a CCS can be expressed as (16).

$$\frac{1}{\sqrt{1-x}} = 1 + \frac{1}{2}x + \frac{1\cdot 3}{2\cdot 4}x^2 + \frac{1\cdot 3\cdot 5}{2\cdot 4\cdot 6}x^3 + \cdots$$
$$= \sum_{k=0}^{\infty}\binom{2k}{k}\Big(\frac{x}{4}\Big)^k = 1 + \sum_{k=0}^{\infty}\binom{2k+1}{k}\frac{1}{2^{2k+1}}x^{k+1} \quad (15)$$

$$X_{CCS}^1 = 8\frac{\varepsilon bw}{\delta}\frac{\delta}{\alpha} \sum_{l=0}^{\infty} \Big(\frac{\alpha}{\delta}\Big)^{2l+2} \frac{1}{2^{2l+1}} \binom{2l+1}{l} \sin\xi\cos\beta$$
$$= 8\frac{\varepsilon bw}{\delta}\frac{\delta}{\alpha}\Big(\frac{1}{\sqrt{1-\big(\frac{\alpha}{\delta}\big)^2}} - 1\Big)\sin\xi\cos\beta \quad (16)$$

Compensation method

Additive nonlinearity of total radial capacitance can be expressed by

$$C - C_{\alpha=0} = \frac{2\pi\varepsilon bw}{\delta}\Big(\frac{1}{\sqrt{1-(\frac{\alpha}{\delta})^2}} - 1\Big) \quad (17)$$

The idea of the compensation method is that the additive nonlinearity is minimized using the measured displacement such as

$$1/Z = \sum_i C_i - a_t\sqrt{X_{CCS}^2 + Y_{CCS}^2} - C_{offset} \quad (18)$$

Here, a_t is a compensation gain, and X_{CCS} and Y_{CCS} are measured displacement with the CCS.

The normalized sum of radial capacitance and the measured normalized displacement are shown in Fig 3. In addition, Figure 3 shows the difference between the sum of radial capacitance and the measured displacement. Considering Eqs. (16) and (19), the optimal compensation gain a can be determined by Eq. (19).

$$\min_a \Big|\Big(\frac{a}{x} - 1\Big)\Big(\frac{1}{\sqrt{1-x^2}} - 1\Big)\Big|_1 \quad (19)$$

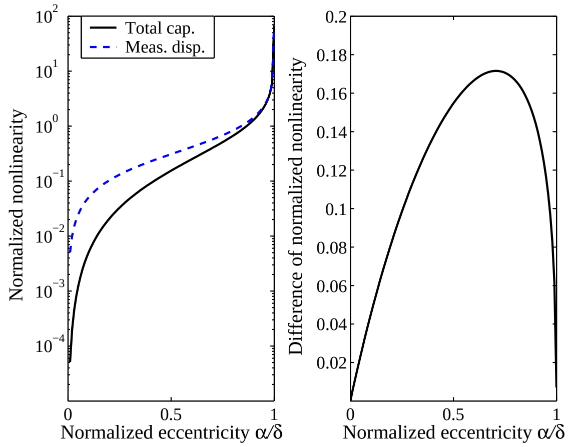

Figure 3: Sum of radial capacitances and measured displacement

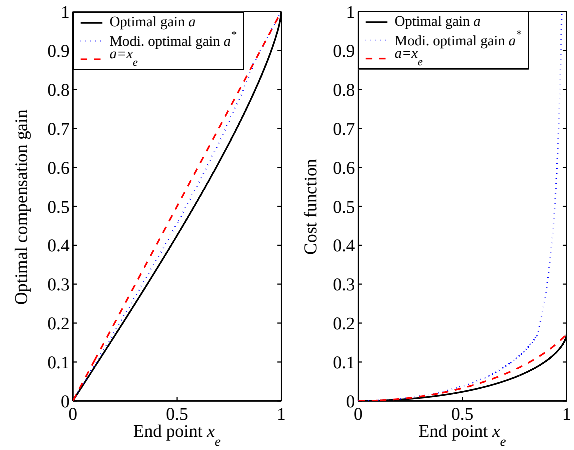

Figure 4: Normalized nonlinearity of the sum of radial capacitances and measured displacement

Here, x is $\frac{\alpha}{\delta}$, $0 \leq x \leq x_e$, $x_e < 1$ and $a = 4a_t \sin\xi/pi$.

Figure 4 shows optimal compensation gains a and with increasing end points x_e. The optimal compensation gain is slightly smaller than the end point. In addition, the cost function values are compared in case the compensation gain is optimal and x_e.

If the rotor is located near the center of the CCS and the compensation error is very small, the proposed compensation equation (18) is too complex and can be simplified by

$$1/Z = \sum_i C_i - a_m(|X_{CCS}|+|Y_{CCS}|) - C_{offset} \quad (20)$$

In the compensation equation above, the eccentricity is approximated as the absolute sum of measured X and Y displacement. However, we have another error source and need to modify the optimal compensation gain into a_m. The maximum error appears in both x and y axis while the minimum error does in both $y = x$ and $y = -x$. The gain a_r can be determined through equalizing the minimum and minimum errors such as

$$\sqrt{2}\, a_r - 1(\text{maximum}) = 1 - a_r(\text{minimum}) \quad (21)$$

The approximation gain a_r is 0.8284 $(2/(1+\sqrt{2}))$ and the relative approximation error is 17.16%.

The cost function should be changed considering the the approximation error such as

$$\min_{a^*} \left|\left(\frac{a^*}{x}-1\right)\left(\frac{1}{\sqrt{1-x^2}}-1\right)\right|_1+\frac{a^*(1-a_r)}{x}\left(\frac{1}{\sqrt{1-x^2}}-1\right) \quad (22)$$

Here, a^* is a_m/a_r.

Through the same procedure as Eq. (19), modified optimal compensation gain a^* and compensation error are calculated and shown in Fig. 4. Although the compensation error using modified compensation equation (20) becomes large as the rotor approaches the CCS, the compensation error is not too severe within $\alpha/\delta < 0.8$.

Error analysis

There are two kinds of intrinsic errors in axial measurement of the proposed CCS: nonlinear harmonic error and compensation error. These two errors result in nonlinearity error of the axial measurement. Figure 5 shows comparison of the biggest normalized nonlinear harmonic error and the normalized compensation errors. The compensation error is much bigger than the nonlinear harmonic errors and the nonlinear harmonic error is ignored in the analysis.

The compensation error results in nonlinear error in axial measurement. If the E_{comp} is the maximum cost function of (18) or (20), the axial measurement can be simplified by

$$\begin{aligned} 1/Z &= \frac{2\pi\varepsilon bw}{\delta}E_{comp} + \frac{2\pi\varepsilon t(b+t/2)}{\delta_a} \\ &= \frac{2\pi\varepsilon bw}{\delta}\left(E_{comp} + \frac{t}{w}\frac{\delta}{\delta_a}\left(1+\frac{t}{2b}\right)\right) \end{aligned} \quad (23)$$

The axial measurement error depends on the CCS geometry including radial thickness, axial width, axial and radial gap. Since $t/2b$ is very small (<<0.1), nonlinear error depends on the ratio of the radial thickness to the axial width t/w. Especially, the

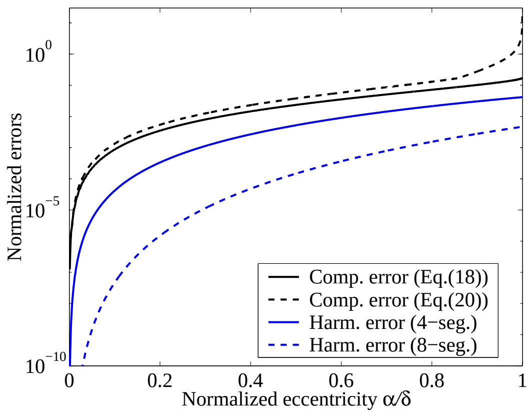

Figure 5: Comparison of normalized nonlinear harmonic and compensation errors

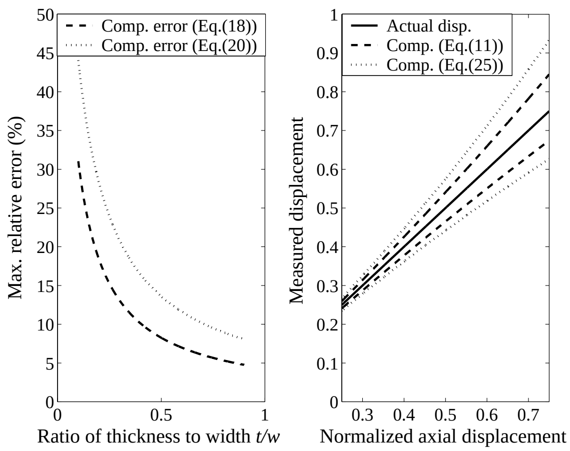

Figure 6: Axial measurement error ($\alpha/\delta \leq 0.75$)

error becomes large as the gap ratio δ/δ_a becomes small, that is, the axial sensing area is farthest.

The relative measured error can be calculated by

$$RE_{axial} = 100\Big(1 - \frac{\frac{t}{w}\frac{\delta}{\delta_a}|_{min}}{E_{comp} + \frac{t}{w}\frac{\delta}{\delta_a}|_{min}}\Big)\ \% \qquad (24)$$

If the normalized eccentricity varies α/δ up to 0.75 and the normalized gap ratio varies from 0.25 to 0.75 (usual AMB application), the maximum relative error with various t/w and measured axial displacement at $t/w = 0.4$ are shown in Fig. .

The rotor radial motion is maintained near center position after the levitation and the normalized eccentricity typically doesn't reach 0.75. If the normalized eccentricity varies up to 0.25 and the normalized gap ratio varies from 0.4 to 0.6 (well-controlled AMB system and precision measurement), the maximum relative error with various t/w and measured

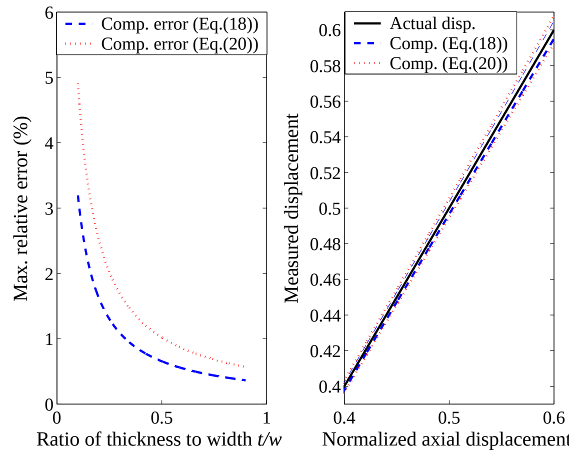

Figure 7: Axial measurement error ($\alpha/\delta \leq 0.25$)

displacement at $t/w = 0.4$ are shown in Fig. 7. The measurement error is very small and the axial motion is measured accurately.

DESIGN RULE

The design principle should be different according to applications and it is a natural thought that the errors of radial and axial measurements are made same. Therefore, it is necessary to evaluate the radial motion measurement error. The nonlinear characteristic of the radial measurement is expressed in (16) and the approximated gain of (16) is '1'. The nonlinear error of the radial measurement can be expressed by

$$RE_{radial} = 100 \cdot \Big(\frac{1}{x^2}\Big(\frac{1}{\sqrt{1-x^2}} - 1\Big) - 1\Big)\% \qquad (25)$$

Here, x is α/δ.

The relative error also increases significantly as the normalized eccentricity increases, as shown in Fig. 8. The relative nonlinear error is about 5% within $\alpha/\delta = 0.25$ and is about 82% within $\alpha/\delta = 0.75$).

In order to equalize the radial measurement error (24) and the axial measurement error (25), the ratio of the radial thickness to the axial width t/w should satisfy

$$\frac{t}{w} = \frac{E_{comp}(x)\Big(2 - \frac{1}{x^2}\Big(\frac{1}{\sqrt{1-x^2}} - 1\Big)\Big)}{\frac{\delta}{\delta_a}|_{min}\Big(\frac{1}{x^2}\Big(\frac{1}{\sqrt{1-x^2}} - 1\Big) - 1\Big)} \qquad (26)$$

Here, x is α/δ.

If the minimum gap ratio δ/δ_a is less than 0.75, the t/w may be less than 0.1, as shown in Figs. and

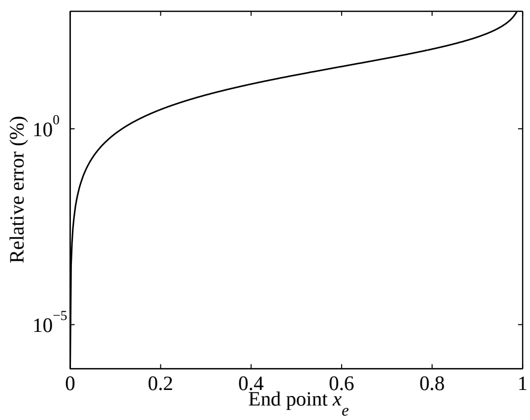

Figure 8: Radial measurement error

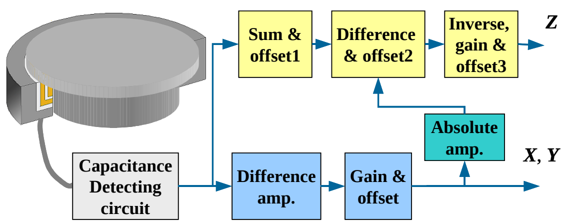

Figure 9: Circuit implementation

7, which means the proposed CCS can measure the axial motion in spite of the small radial thickness within comparable accuracy.

CIRCUIT IMPLEMENTATION AND CALIBRATION

A circuit block diagram for the proposed CCS is shown in Fig. 9. The proposed CCS use the same circuit as the existing CCS in the radial measurement: capacitance detecting circuit, difference amplifier and gain & offset adjustment. The nonlinear relationship between capacitance and displacement is approximated using simple difference amplifier. In addition, the center of the CCS is set electrically through making the CCS radial output zero without a target using the offset adjustment circuit.

On the other hand, the axial measurement circuit consists of three stage: sum & offset1, difference & offset and inverse, gain & offset3. First, all capacitances are summed and stray capacitance effect are removed though making the first stage output zero without a target using offset1 circuit. Second, the radial dependency is compensated through subtracting the absolute sum of measured radial measurements. In addition, the sum of radial capacitance is removed through making the second stage output zero with only radial target using offset2 circuit. Finally, the second stage output is inversed and the output signal is adjusted.

The proposed CCS measures both radial and axial motion. Therefore, the CCS should be calibrated in both X, Y and Z directions at the same time. The calibration procedure of the CCS is as follows: First, offsets of the proposed CCS are set electrically through making the some stage outputs zero with or without a target. The sensor output is measured moving an alternative target with the same diameter as the rotor in both X, Y and Z direction. The calibration results will be presented in conference presentation.

CONCLUSION

This paper proposed a novel cylindrical capacitive sensor (CCS) for both radial and axial motion measurement. unused axial area of the CCS is adopted to measure the axial motion of a rotor. Although the radial motion of the rotor affects measurement of the axial motion significantly due to the intrinsic nonlinear characteristic of CCS, a simple compensation method to decouple the radial and axial motion measurements is proposed. In addition, error analysis of the CCS is performed and a design rule is developed to guarantee the same accuracy in measuring both radial and axial motion measurements. Finally, a test rig and electronics for the proposed CCS are built and the performances of the proposed CCS is verified experimentally. The proposed CCS can reduce complexity of the hardware configuration and offer more degree of freedom in design.

ACKNOWLEDGMENT

This work was supported by the Brain Korea 21 Project in 2004

REFERENCES

[1] Ahn, H. J., Jeon, S., Han, D. C., 2000, "Error analysis of the cylindrical capacitive sensor for active magnetic bearing spindles," *Journal of Dynamics systems, measurement, and control, trans. of ASME*, Vol. 122, pp.102-107.

[2] Jeon, S., Ahn, H. J., Chang, I. B. and Han, D. C., 2001, "A New Design of Cylindrical Capacitive Sensor for On-line Precision Control of AMB Spindle", *IEEE Transactions on Instrumentation and measurement*, Vol. 50(3), pp. 757-763.

[3] Gradshteyn, I. S. and Ryzhik, I. M. , 1982, *Table integrals, series, and product*, Academic press, Inc..